

**EFFECT OF GEOGRID ORIENTATION FOR CONE  
PENETRATION RESISTANCE OF SAND USING NUMERICAL  
AND ANALYTICAL MODELLING**

A PROJECT REPORT

SUBMITTED IN PARTIAL FULFILLMENT OF THE REQUIREMENTS

FOR THE AWARD OF THE DEGREE

OF

MASTERS OF TECHNOLOGY

IN

GEOTECHNICAL ENGINEERING

Submitted by:

**DEEPANSHU**

**2K18/GTE/07**

Under the supervision of

**PROF. ASHUTOSH TRIVEDI**



**DEPARTMENT OF CIVIL ENGINEERING**

DELHI TECHNICAL UNIVERSITY

(Formerly Delhi College of Engineering)

Bawana Road, Delhi-110042

JUNE, 2020

# DELHI TECHNICAL UNIVERSITY

(Formerly Delhi College of Engineering)

Bawana Road, Delhi-110042

## CANDIDATE'S DECLARATION

I, **Deepanshu, 2K18/GTE/07**, student of M.Tech, Geotechnical Engineering, hereby declare that the project Dissertation titled “**EFFECT OF GEOGRID ORIENTATION FOR CONE PENETRATION RESISTANCE OF SAND USING NUMERICAL AND ANALYTICAL MODELING**” which is submitted by me to the Department of Civil Engineering, Delhi Technical University, Delhi in partial fulfillment of the requirements for the award of the degree of Master of Technology, is original and not copied from any source without proper citation. This work has not previously formed the basis for the award of any Degree, Diploma Associateship, Fellowship, or other similar title or recognition.

Place: Delhi

Date:

DEEPANHU

**DEPARTMENT OF CIVIL ENGINEERING**

**DELHI TECHNICAL UNIVERSITY**

(Formerly Delhi College of Engineering)

Bawana Road, Delhi – 110042

**CERTIFICATE**

I hereby certify that the Project Dissertation titled “**EFFECT OF GEOGRID ORIENTATION FOR CONE PENETRATION RESISTANCE OF SAND USING NUMERICAL AND ANALYTICAL MODELING**” which is submitted by DEEPANSHU, 2K18/GTE/07, Department of Civil Engineering, Delhi Technical University, Delhi in partial fulfillment of the requirement for the award of the degree of Master of Technology, is a record of the project work carried out by the students under my supervision. To the best of my knowledge this work has not been submitted in part or full for any Degree or Diploma to this University or elsewhere.

Place: Delhi

**PROF. ASHUTOSH TRIVEDI**

Date:

**SUPERVISOR**

## ACKNOWLEDGEMENT

I express my profound gratitude and have no words to reveal my gratefulness to Prof.Ashutosh Trivedi, Department of Civil Engineering, Delhi Technical University, Delhi, whose able guidance and provoking of encouragement has been the great force that enabled me to prepare this project report on the topic “**EFFECT OF GEOGRID ORIENTATION FOR CONE PENETRATION RESISTANCE OF SAND USING NUMERICAL AND ANALYTICAL MODELING**”. He devoted considerable time in guiding and checking my work and made valuable suggestions.

I am grateful to Prof.NirendraDev, Head of the Civil Engineering Department for the facilities provided to carry on the work. I am thankful to all the faculty members of Geotechnical Engineering for their cooperation and moral support and to all those who helped me in making this project better by providing their valuable comments and guidance.

I would also like to thank my parents and lab assistants who helped me in performing the project work within the limited time frame.

DEEPANSHU

(2K18/GTE/07)

## ABSTRACT

In the present study, the problem of low resistance offered by the soil to penetration is solved to a great extent by reinforcing the soil with geogrid. The results of the cone resistance vs penetration were observed to be dependent on the orientation of geogrids. The geogrids were reinforced at bottom of the container and depth of 5.5cm and 11cm in the horizontal direction. The cone resistance is determined at the densities of 1.54 g/cc, 1.59 g/cc, and 1.65 g/cc respectively of soil. Nine experimental data set values led us to the conclusion that the best cone resistance was offered at the maximum dry density and the water content being at optimum moisture content. When geogrids being reinforced at bottom of the container and a depth 11 cm of the soil layer, the cone resistance was observed to be 3.6 times higher than that obtained in the case when the soil was not reinforced. 1.2 times higher cone resistance was observed than that when the geogrids are reinforced in three layers of the soil.

The analytical results were analyzed with a numerical modeling program. The results were validated by performing numerical modeling against the field results. A dimensionless cone penetration resistance factor (DCPRF) led us to the validation of the numerical model. DCPRF relates the ratio of cone penetration resistance obtained in the analytical modeling with the numerical modeling. DCPRF converges to unity as the value of the factored load is increased. DCPRF in sand reinforced with geogrid has more importance than cone penetration alone observed in the literature.

# CONTENT

## PAGE NO.

Declaration	ii	
Certificate	iii	
Acknowledgement	iv	
Abstract	v	
List of Figures	viii	
List of Tables	x	
Chapter 1	Introduction	1
	1.1 Cone penetration test	1
	1.2 Geogrid	2
	1.3 FEM	4
Chapter 2	Literature review	5
Chapter 3	Experimental Setup	7
	2.1 Geometric model of testing mould	7
	2.2 Static cone penetrometer and LVDT	8
	2.3 Polyethylene geogrids	11
Chapter 4	Observations and Calculations	13
	4.1 Sieve Analysis	13
	4.2 Direct Shear test	15
	4.3 Proctor test	16

	4.4 Static cone Penetration Test	18
	4.5. Tabular form of Cone resistance with varying densities and varying orientation of geogrid	23
Chapter 5	Software Modelling	24
	5.1. Objective	25
	5.2. Model Preparation	25
	5.3. Modelling Analysis	26
	5.4. The table of comparison of results in numerical modelling and analytical modelling and its related Graphs	35
Chapter 5	Conclusion	38
Chapter 6	Future Scope	39
References		

## LIST OF FIGURES

S. No	Title of figure	Page no.
Figure 1	Biaxial square geogrid	3
Figure 2	Section of mold	7
Figure 3	Static cone penetrometer	8
Figure 4	Data process analoger	9
Figure 5	Cones of the static cone penetration test	9
Figure 6	Cross-section of Static cone penetrometer (IS:4968 ( Part II ) – 1976)	11
Figure 7	sieve analysis	13
Figure 8	Particle size distribution curve	14
Figure 9	Direct shear test apparatus	15
Figure 10	The plot of shear stress Vs normal stress	16
Figure 11	The plot of density Vs water content in the Proctor test	17
Figure 12	Cone penetration resistance profiles at a density of 1.54 g/cc with different reinforcement orientations of geogrid	18
Figure 13	Cone penetration resistance profiles at a density of 1.59 g/cc with different reinforcement orientations of geogrid	19
Figure 14	Cone penetration resistance profiles at a density of 1.65 g/cc with different reinforcement orientations of geogrid	20
Figure 15	Cone penetration resistance profiles in the sand without the reinforcement of geogrid at different density	21
Figure 16	cone resistance profiles in the sand with reinforcement of geogrid in the horizontal direction at the top layer, middle layer and bottom layer of soil layer at different density	22
Figure 17	cone resistance profiles in the sand with reinforcement of geogrid in the horizontal direction at the top layer and bottom	22



	layer of the soil layer at a different density.	
Figure 18	A 15 noded Axis-symmetry model generated mesh	26
Figure 19	A soil element without geogrid reinforcement	26
Figure 20	A plot of vertical displacement for a soil element without geogrid reinforcement	27
Figure 21	A plot of cone penetration resistance for a soil element without geogrid reinforcement	28
Figure 22	A soil element with a two-layer geogrid reinforcement	29
Figure 23	A plot of vertical displacement for a soil element with a two-layer geogrid reinforcement	30
Figure 24	A plot of cone penetration resistance for a soil element with a two-layer geogrid reinforcement	31
Figure 25	A soil element with a three-layer geogrids reinforcement	32
Figure 26	The plot of a deformed mesh for a three-layer geogrid reinforced soil element	33
Figure 27	A plot of vertical displacement for a soil element with a three-layer geogrid reinforcement	33
Figure 28	A plot of cone penetration resistance for a soil element with a three-layer geogrid reinforcement	34
Figure 29	Comparison of load Vs displacement for numerical and analytical modeling for different orientation of geogrid reinforcement	35
Figure 30	Comparison of load Vs cone penetration resistance in numerical and analytical modeling for different orientation of geogrid reinforcement	36
Figure 31	Comparison of load Vs DCPRF in numerical and analytical modeling for different orientation of geogrid reinforcement	37

## LIST OF TABLES

<b>Table no</b>	<b>Table title</b>	<b>Page no</b>
Table 1	Geogrid Properties (Shinoda.M and Bathurst.R.J, (2004)	12
Table 2	Sieve analysis	13
Table 3	Direct Shear test	15
Table 4	Proctor Test	16
Table 5	Cone penetration resistance with varying densities and varying orientation of geogrid	23
Table 6	The tabular form of Load and Displacement in numerical and analytical modeling	35
Table 7	The tabular form of Load and cone penetration resistance in numerical and analytical modeling	36
Table 8	The tabular form of Load and DCPRF	37

# CHAPTER 1

## INTRODUCTION

Cone penetration in the sand with geogrids is a much complex problem. The problem arises since the penetration resistance offered by the sand is significantly less at low densities and penetration is very high.

In testing of soil beds, the most effective and the best method is the cone penetration test. This consists of collecting a bulk volume of data on the properties of soils at various depths under various conditions and different stratification of soil, including those prevalent on the continental base. Several empirical and experimental methods have been suggested to obtain soil properties and parameters of the penetration resistance. These approaches have been established for the determination of soil properties. The determination of cone resistance test results is normally based on a calibration chamber study with controlled conditions of density and overburden. (Ahmadi, Byrne and Campanella et. al 2005)

### 1.1 Cone Penetration Test (CPT)

Static Cone penetrometer test (CPT) is a useful method when used simultaneously with various other procedures in the analysis of engineering structures. The details of various equipment of a cone penetrometer test and steps to be followed in conducting the tests are texted below. Consistency in all parts of cone penetrometer testing is the need.

A few penetrometers of different sorts were utilized in the Netherlands and Scandinavia starting around 1900. A cone penetrometer combined with a sleeve or shield first experimented in Holland in 1936. In 1946, the Dutch cone was produced by Goudsche Machinefabriek of Gouda, first as 2500 kg limit mechanical assembly. A couple of years after, this organization started making equipment of 10000 kg and 2000 kg limit. One of the numerous points of interest of static cone penetrometer is the capacity to separate, or expel, the obscure contact powers that create on the push holes. In static penetrometer testing, just the resistance from the cone point and contact sleeve estimated.

Mostly static penetrometer test consists of a drill rig that is inserted into the ground and pushed below with the help of hydraulic jacks. These hydraulic jacks also help in retrieving these rigs. Truck-mounted penetrometer rigs that are self-contained in a small space are also available.

In regions where engineering parameters of soil are known earlier, their static cone penetration tests help to make accurate estimates of settlements and shear strength of underground soil. Since both static and dynamic testing is available, it can be that samples to be tested are to be completely relied upon as they can be disturbed or may even become irretrievable.

These tests are currently in use by SCS in Iowa, Kansas, and Nebraska. Various penetrometers are applied in Midwest by the Corps of Engineers and associated engineering companies. Cone penetrometers were first used by SCS in May 1974.

The penetrometer that is commonly used is a cone with an apex angle of  $45^\circ$  and  $60^\circ$  with a base area of  $9.62 \text{ cm}^2$ .

## 1.2. Geogrid

Geogrid is a major type of geo-synthetics which has been employed successfully for soil reinforcement. The two common types of geogrids are uniaxial and biaxial geogrids. Uniaxial geogrid has the tensile strength in one direction while biaxial geogrid has tensile strengths in two directions (i.e., machine and cross-machine directions). Uniaxial geogrid finds its application in retaining walls, reinforcing slopes, and embankments, whereas biaxial geogrid is normally used stabilizing roadways including paved roads, unpaved roads and railroads. Research on the use of geogrid and its related field applications have shown that a properly designed and oriented geosynthetic does improve the performance of roads.

These grids are composed of material ribs that are crossed or intersected in two directions during the process of manufacturing. One direction is the machine direction which as the name suggests is in the direction the same as that of manufacturing. The other direction is perpendicular to this and is known as cross-machine direction (CMD). Amongst various geotextiles, geogrids are considered much harder and stiffer. In geogrids stresses due to loads are transferred through these junctions hence strength at a junction is essential for them to function properly. Aggregates are being held up or captured together through geogrids. Through this interlocking of aggregates, the earthquake becomes stabilized mechanically.

The longitudinal and transverse ribs of Geogrid forms apertures. Biaxial geogrid has rectangular square or triangular apertures. Geogrid apertures helps in the interlocking of aggregates. This interlocking between geogrid and aggregate helps to form a confined zone above and below the geogrid if an appropriate relationship between the aperture size of the geogrid and the particle

size of the aggregate exists. The biaxial geogrids have higher stiffness and tensile strength and in their machine and cross-machine directions, but much lower stiffness and strength in other directions, especially at an angle of  $45^\circ$  in the loading direction.



Figure 1: Biaxial square geogrid

### Types of Geogrids

Based on the manufacturing process involved in the construction of geogrids it can be classified as

1. Extruded Geogrid
2. Woven Geogrid
3. Bonded Geogrid

Based on the direction of stretching adopted during the manufacturing process it can be classified as

1. Uniaxial Geogrids
2. Biaxial Geogrids

### Uniaxial Geogrid

These types of geogrids are formed by the expansion of ribs in the direction the same as that of machining i.e. in the longitudinal direction. Hence in uniaxial geogrids, tensile strength is higher in a longitudinal direction and is lower in the direction at the right angle to it i.e. in the transverse direction.

### Biaxial Geogrids

In this case during the process of punching polymeric sheets, stretching or expansion of grids is carried out in both the directions. Hence tensile strength is equal in both longitudinal as well as transverse direction.

The use of soil with geogrid reinforcement brings quality and the cost of construction is also reduced

### 1.3.FEM

The finite element method (FEM) is a method of problem-solving which can be formulated as functional minimization or described by partial differential equations.

A discrete finite element problem is transformed from a continuous physical problem with unknown number of nodal values.

Two properties of the FEM that are to be mentioned:

1) Node-wise analysis of physical fields on finite elements provides good accuracy even with simple approximating and analytical functions.

2) The position of approximation leads to scanty equation systems for a discrete problem. This helps to resolve problems with a large number of nodal unknowns.

#### 1.3.1. Plaxis 8X

Plaxis a finite element software that has been developed especially for the analysis of stability and deformations in geotechnical engineering. It is a simple graphical method in which the input processes allows a generation of complex finite element

Models and the output analysis provides for the easy computation of results. The calculation is based on fully automatic numerical methods

## **CHAPTER 2**

### **Literature review**

Literature review of the research papers used in this study are as follows:

**Paper 1:** Performance of triangular aperture Geogrid-Reinforced Base courses over weak subgrade under cyclic loading

Authors: Qian and Han(2013)-Geogrid (uniaxial or biaxial) are the types of geosynthetics that has been successfully used in walls, roads, slopes, and other applications. The experimental and theoretical research has revealed that biaxial geogrid are unable to provide uniform or a constant tensile resistance to load in all the directions. Recent studies stated that the geogrids of triangular aperture provides for a next to uniform tensile resistance in all directions and is much more efficient in enhancing the performance of reinforced surfaces as compared the same with biaxial geogrid. The test results indicates that a triangular aperture geogrids decreases permanent deformation and maximum vertical stress at the interface as compared with that of unreinforced bases.

**Paper 2:** Strain measurement of Geogrids using a video-extensometer technique

**Authors:** Shinoda M and Bathurst RJ (2004) ASTM

There is also be a technique to determine displacements and local strains at the surface of a typical geogrid reinforcement using a video-extensometer. Local axial reinforcement strains for uniaxially drawn HDPE geogrids are non-uniform at large axial strains.

**Paper 3:** Cone tip resistance in the sand: Modeling, Verification, and Applications

**Authors:** Ahmadi MM, Byrne PM and Campanella RG (2004) NRC Canada

The cone-tip resistance in the sand can also be analysed using numerical modeling. The method involves a moving boundary simulating cone penetration. The soil modelling is done using a Mohr-Coulomb elastic-plastic material with stress-dependent parameters. The discrete program FLAC is used to carry out its analysis. The test of a sensitivity analysis revealed that the cone resistance is a measure of soil modulus. With the increase in tip resistance, the soil modulus increases. Dilation angle is also important, with the higher values of dilation angles resulting in higher tip resistances.

**Paper 4:** Cone resistance of compacted ash fill

**Authors:** Trivedi A and Singh S (2004) ASTM

The cone resistance test when performed on coal ash revealed the use of bearing capacity factors as per the magnitude of cone resistance and density. The settlement was found to be higher when calculated with the conventional methods of a plate load test. Thus a modified relation was obtained based on the cone penetration test to obtain the penetration of the ash fill.

**Paper 5:** Large displacement FEM modeling of the cone penetration test(CPT) in normally consolidated sand

**Authors:** Susila and Hryciw(2003) John Willey and Sons Ltd

An auto-adaptive re-meshing finite element model has been presented for the study of cone penetration into normally consolidated sands using. The study shows that avoids numerical problems that would otherwise develop due to the high distortion of soils surrounding the cone tip. The other significant improvements are the modeling of a special boundary which prohibits soil from displacing across the axis-symmetric centerline; and the infinite elements at the periphery of the model. Drucker–Prager constitutive model was used to model sand

In dense sand, tip resistance ( $q_c$ ), the soil within a 600–800 mm zone above and below the cone tip is affected while in loose sand this zone of affected soil zone approximately 180–260 mm.

**Paper 6:** Effect of particle size distribution on pile tip resistance in calcareous sand in the geotechnical centrifuge

**Authors:** McDowell GR and Bolton MD (2000) Springer

particle size distribution helps in determining the constitutive behavior of soil. The paper reveals the boundary problem of the penetration of the model pile into two different gradings of soil. The different grading of soil used is dry calcareous sand of particles smaller than 0.5mm and second grading of particles of size ranging from 0.15 mm to 0.5mm in a geotechnical centrifuge. Tip resistance of soil rises to the peak and then fall at shallow depth. To conclude, The penetration resistance of sands depends on the initial condition and properties of soil mass (relative density and pre-existing stress level) being penetrated and also on a complex function of soil compressibility and penetration geometry.



## CHAPTER 3

### Experimental Setup

#### 3.1. Geometric model of a testing mold

A testing model of a mold of size 29.2cm X 12.6cm X 20 cm was constructed of steel plates having a thickness of 3mm. The soil is placed in the mold at a fixed height. The tank is made up of a steel plate at the bottom and one side of the tank is made up of an acrylic sheet of thickness 15mm on one side. The acrylic sheet is provided to observe the failure pattern of the soil in the mold.



Figure 2: Section of mold

### 3.2. Static cone penetrometer and LVDT

This is an instrument that can be used to measure both loads acting at the tip of the penetrometer and also the displacement at the tip through the use of LVDT (linear variation digital transformer). Cones of various sizes can be attached to the tip to find the load or resistance acting at the tip of the cone. Displacement can be measured through a narrow stick which is attached to LVDT. This apparatus can be connected with a data logger which is used to record the variation of both displacement and load at the tip of the static cone penetrometer. A pen drive can be attached to this data logger to extract the readings. The cone used was of 1.75 cm radius and  $45^\circ$  apex angle cone.



Figure 3: Static cone penetrometer



Figure 4: Data process analog gear



Figure 5: Cones of a static cone penetration test

## Equipment

1. Cone- the cone shall be of suitable steel hardened tip. The cone should be suitably threaded to enable it to be attached to a rod used for driving.
2. Driving rods – the rods used for the test should be of suitable length and be marked at suitable intervals.

3. Driving head- it shall be of mild steel with threads at either end.
4. Hoisting equipment- any suitable hoisting equipment like a tripod may be used. The equipment shall be designed to be stable under the impact of a load when the cone is driven during the test.

Procedure( IS:4968 ( Part II ) – 1976)

1. Position 1- The cone and the friction jacket assembly is in a stationary position
2. Position 2- The cone is pushed into the soil by the inner sounding rod to a depth a, at a steady rate of 20mm/s, till a collar engages the cone. The tip resistance  $q_c$  called the point of the cone resistance can be calculated by the force  $Q_c$  read on the digital meter.
3. Position 3- The sounding rod is pushed further to a depth b. This has the effect of pushing the friction jacket and the cone assembly together. The total force  $Q_t$  is again read on the digital meter. The force required to push the friction jacket along with  $Q_f$  is then obtained as  $Q_t - Q_c$ . the side and the skin friction is equal to  $\frac{Q_f}{A}$  where A is the area of the friction jacket.
4. Position 4- The outside mantle tube is pushed down to a distance (a+b), bringing the cone and friction jacket to position 1.

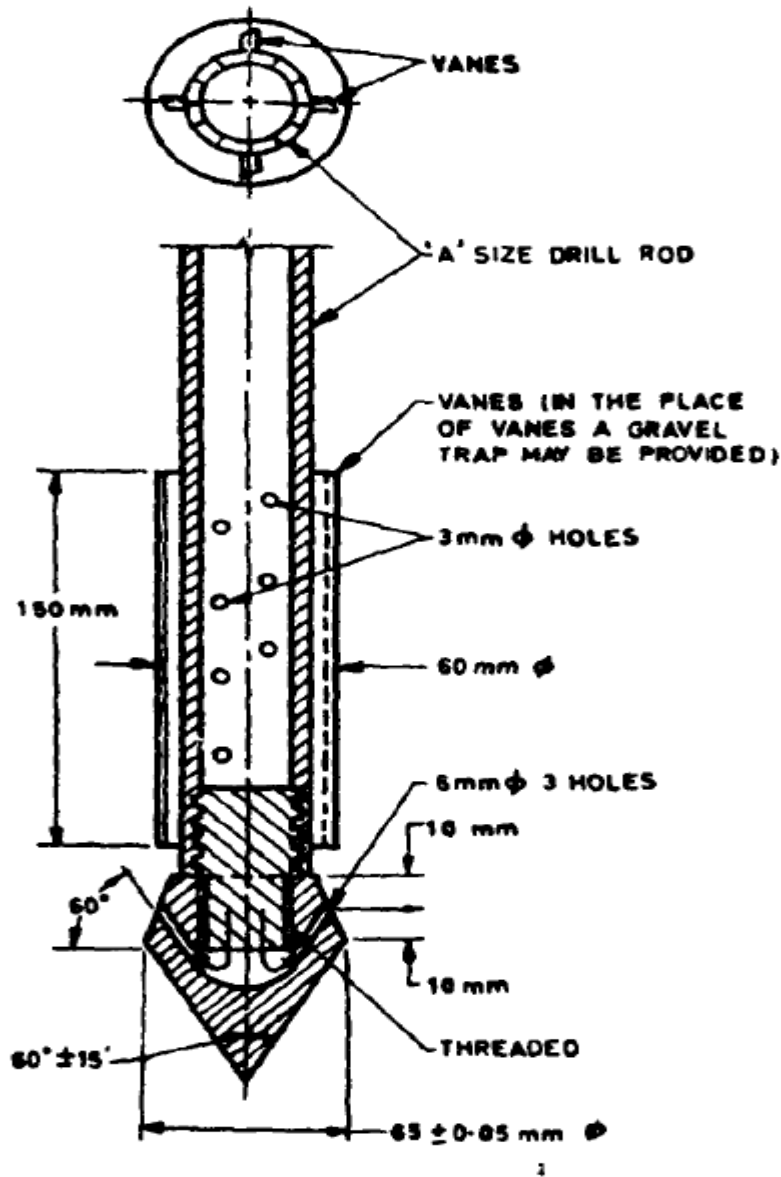


Figure 6: Cross-section of Static cone penetrometer (IS:4968 ( Part II ) – 1976)

### 3.3. Polyethylene geogrids

Specimens of biaxial polypropylene (PP) geogrid, knitted polyester (PET) geogrid, and uniaxial high-density polyethylene (HDPE) geogrid were used in the current investigation. These materials are typical geogrid reinforcement products used in soil reinforcement applications. The properties of this geogrid are illustrated as:

Table 1: Geogrid Properties (Shinoda.M and Bathurst.R.J, (2004)

Property	
Structure	HDPE Punched sheet and drawn
Coating	Uncoated
Mass/unit area(g/m <sup>2</sup> )	NA
Aperture size(mm)	
Machine direction	140
Cross-machine direction	15
Thickness(mm)	
A longitudinal member	1
At junction	2.7
Wide-width tensile strength(KN/m)	
At 5 % strain	35.7
Ultimate	68.9

# CHAPTER 4

## OBSERVATIONS AND CALCULATIONS

### 4.1.Sieve analysis

SIEVE SIZE	% FINER
4.75	98.8
2.36	98.4
1.18	96.7
0.6	95.4
0.3	44.7
0.15	13.6
0.075	2.2
Pan	0.3

Table 2: Sieve analysis



Figure 7: sieve analysis

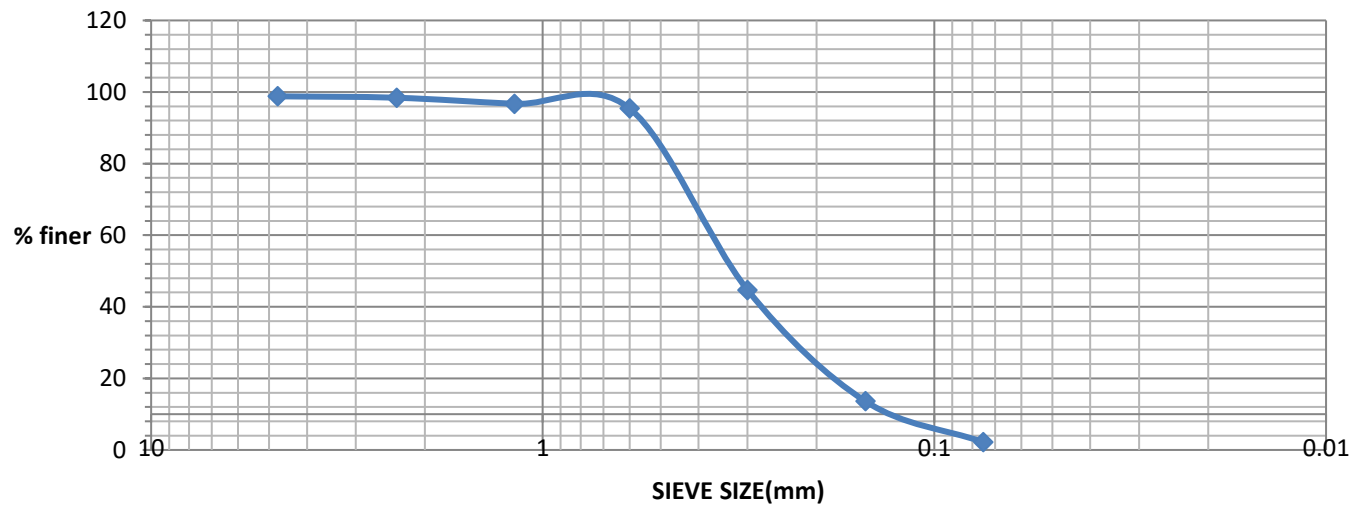


Figure 8: Particle size distribution curve

According to IS Code % passing through 0.075mm sieve is less than 50% hence it is coarse-grained soil.

Since sand fraction ( $0.075\text{mm} < d < 4.75\text{mm}$ ) > Gravel fraction ( $d > 4.75$ )

Hence it is classified as Sand.

From the particle size distribution curve

$D_{60} = 0.4\text{mm}$

$D_{30} = 0.21\text{mm}$

$D_{10} = 0.15\text{mm}$

Coefficient of Uniformity,  $C_u = \frac{D_{60}}{D_{10}} = 2.67$

Coefficient of Curvature,  $C_c = \frac{D_{30} * D_{30}}{D_{60} * D_{10}} = 0.735$

Hence it is a Poorly Graded Sand (SP)



#### 4.2. Direct shear test



Figure 9: Direct shear test apparatus

NORMAL STRESS (KN/m <sup>2</sup> )	SHEAR STRESS (KN/m <sup>2</sup> )
50	4.672
100	9.742
150	13.607

Table 3: Direct Shear test

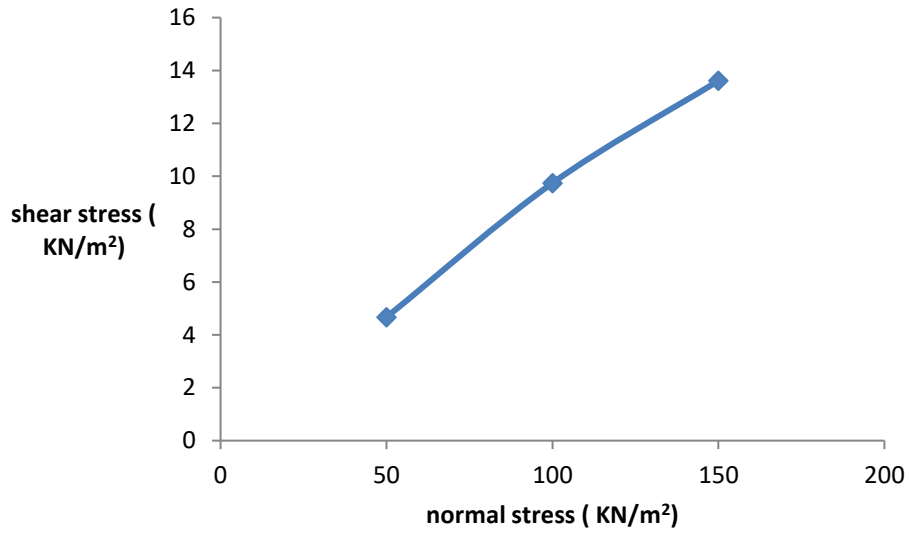


Figure 10:Plot of shear stress Vs normal stress

From the direct shear, it can be concluded that

Cohesion,  $C=4.05 \text{ KN/m}^2$

The angle of internal friction= $41.78^\circ$

#### 4.3.Proctor test

WATER CONTENT	DENSITY (g/cc)
8.1	1.62
9.6	1.69
10.3	1.56

Table 4: Proctor Test

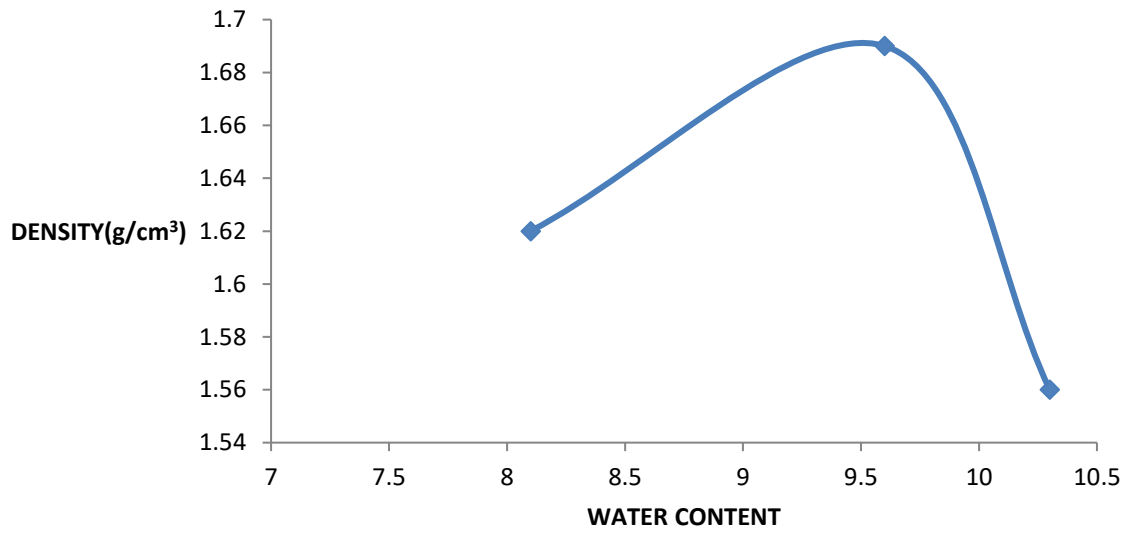


Figure 11: Plot of density Vs water content in the Proctor test

Optimum moisture content =9.6%

Maximum dry density= 1.69 g/cc

#### 4.4. The static cone penetration test

The static cone penetration test was carried out at a different density of 1.54 g/cc, 1.59 g/cc, and 1.65 g/cc. Firstly the unreinforced soil (sand) was used at these varying densities. Secondly, the soil was reinforced with geogrids provided at a different orientation in the horizontal direction with the geogrids reinforced in three layers that are the top, middle, and the bottom layer of the soil; called as three-layer reinforcement and then thirdly, the soil is reinforced in two layers that are the top and the bottom layer; called as a two-layer reinforcement.

4.4.1. The plot of cone resistance vs depth at a density of 1.54 g/cc with different orientation of geogrid

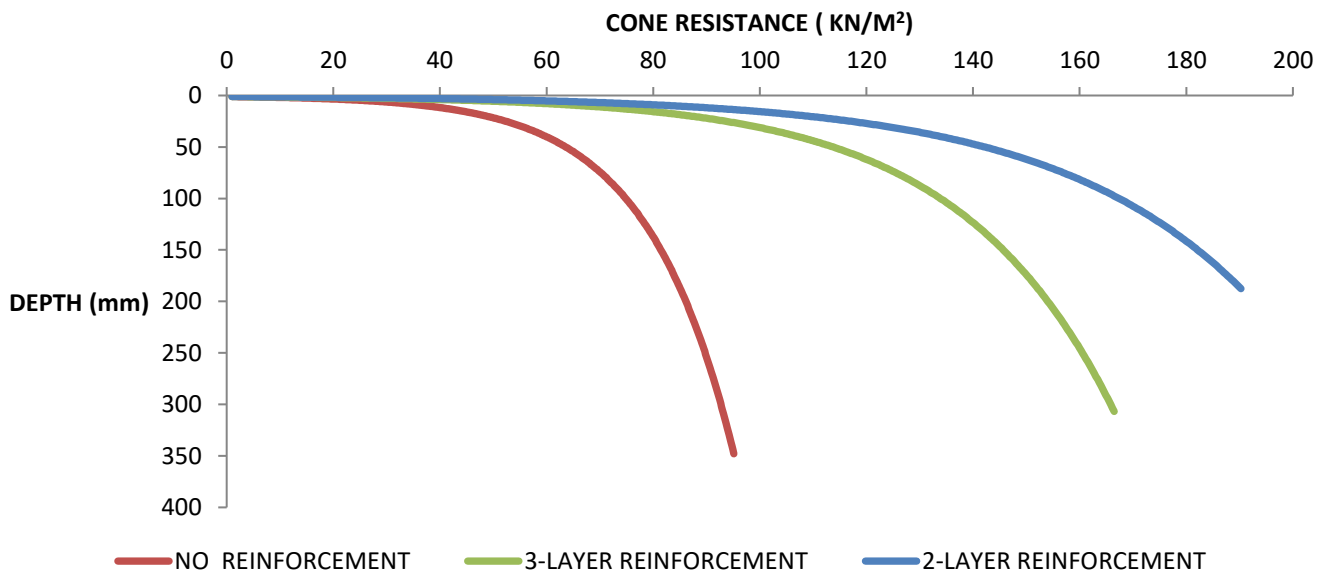


Figure 12: Cone penetration resistance profiles at a density of 1.54 g/cc with different reinforcement orientations of geogrid

Result: As being observed from the graph, for a minimum depth of penetration, the cone resistance is highest when the soil is reinforced in two layers that are at the top and bottom layer of the soil and is approximately twice to that of soil without reinforcement and is approximately 1.1 times to that when the soil is reinforced in three layers.

4.4.2. The plot of cone resistance vs depth at a density of 1.59 g/cc with different orientation of geogrid

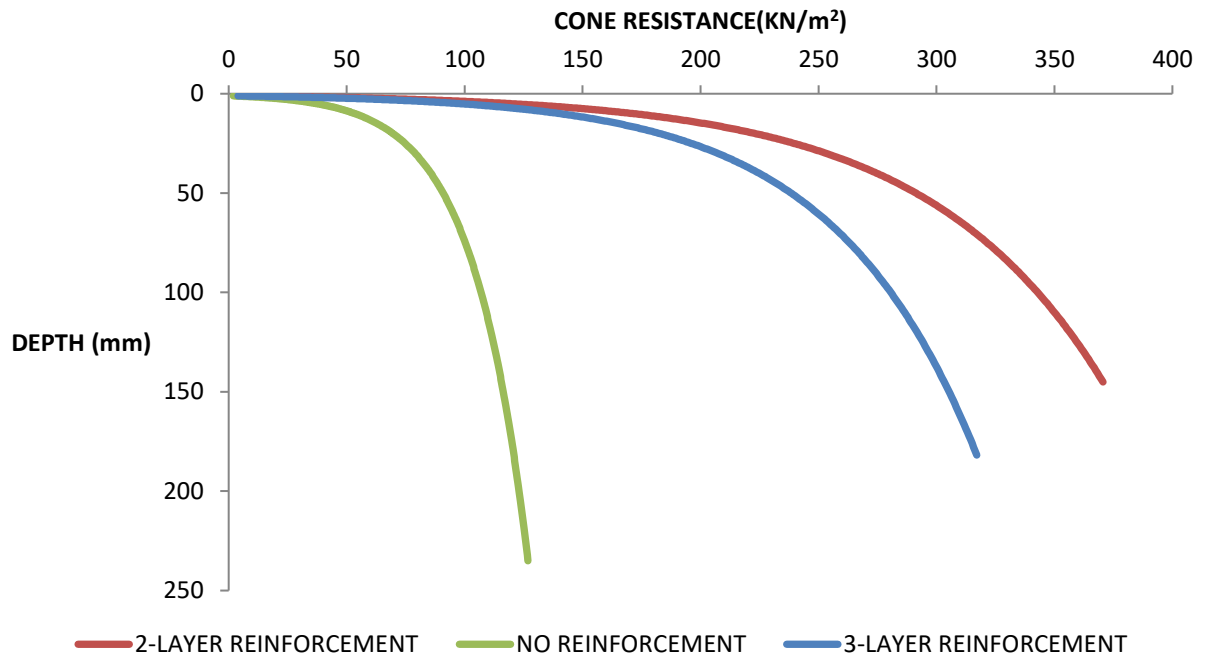


Figure 13: Cone penetration resistance profiles at a density of 1.59 g/cc with different reinforcement orientations of geogrid

Result: As being observed from the graph, the cone resistance is highest when the soil is reinforced in two layers that are at the top and bottom layer of the soil and is approximately thrice to that of soil without reinforcement and is again approximately 1.1 times to that when the soil is reinforced in three layers as in the previous case when the density of soil was 1.54 g/cc.

4.4.3. The plot of cone resistance vs depth at a density of 1.65 g/cc with different orientation of geogrid

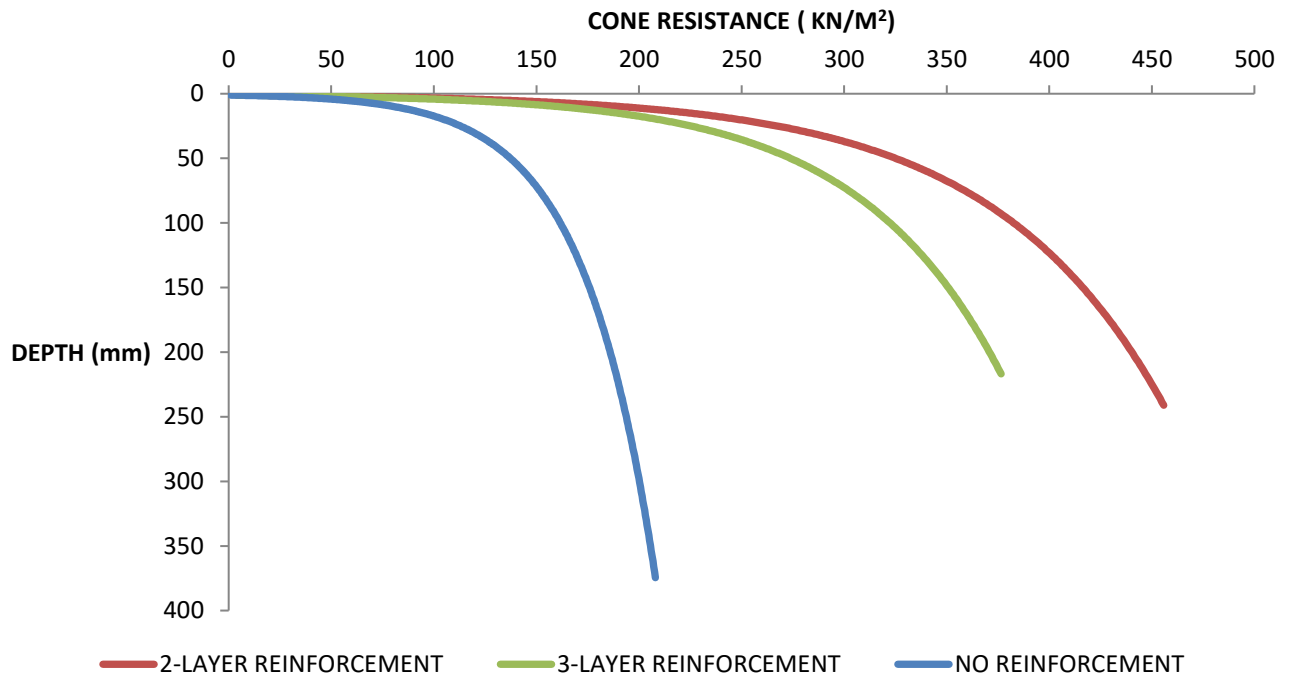


Figure 14: Cone penetration resistance profiles at a density of 1.65 g/cc with different reinforcement orientations of geogrid

Result: The cone resistance is highest when the soil is reinforced in two layers that are at the top and bottom layer of the soil but with a little more depth of penetration than the case when the soil was reinforced in three layers and this value of cone penetration resistance is approximately 2.2 times to that of soil without reinforcement and is again approximately 1.2 times to that when the soil is reinforced in three layers with geogrid.

4.4.4. The plot of cone resistance vs depth in the sand without the reinforcement of geogrid at different density

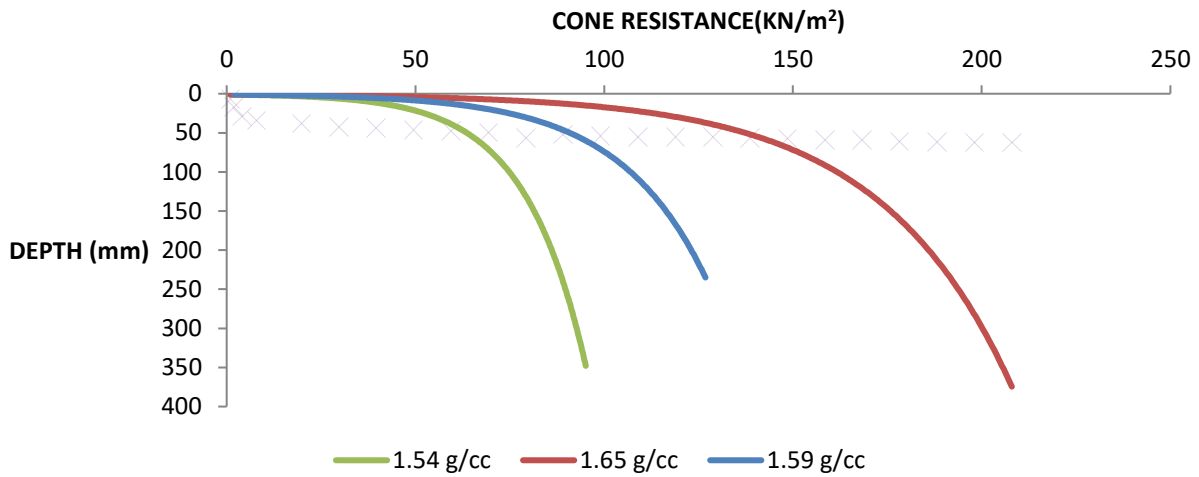


Figure 15: Cone penetration resistance profiles in the sand without the reinforcement of geogrid at different density

Result: The highest cone resistance in the soil without reinforcement is at the density of 1.65g/cc. As concluded, with the increase in density, the cone penetration resistance increases and this increase is also significant concerning the other two densities of 1.54g/cc and 1.59 g/cc.

4.4.5. The plot of cone resistance vs depth in the sand withgeogrid reinforcement in three layers in the horizontal direction that is at the top of the container, middle depth of container and bottom of the container of soil at different density

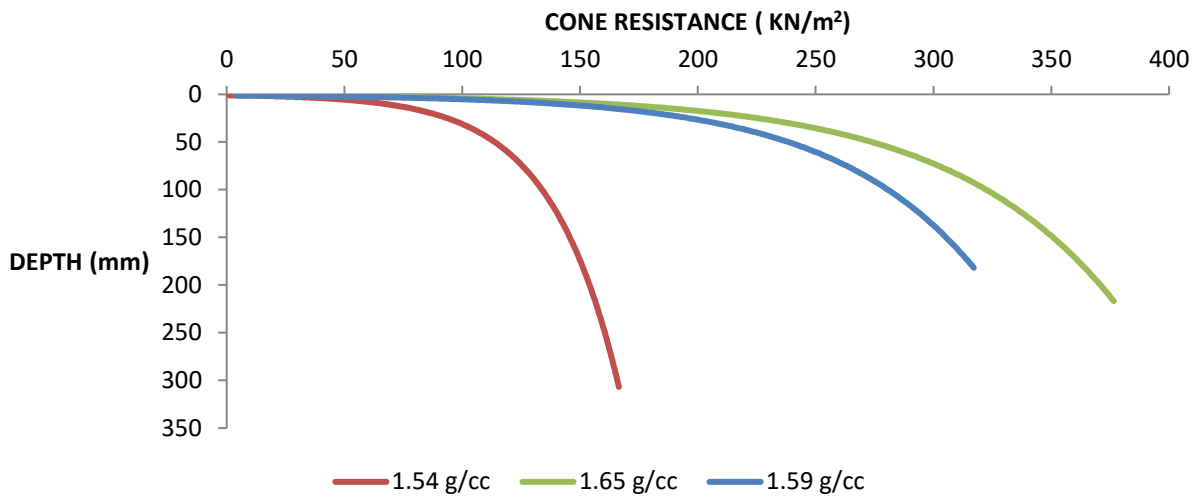


Figure 16: cone resistance profiles in the sand with reinforcement of geogrid in the horizontal direction at the top layer, middle layer and bottom layer of soil layer at different density

Result: With the geogrids reinforced at the top, middle and bottom layers of the soil, the highest cone resistance appears out to be for the soil of highest density

4.4.6. The plot of cone resistance vs depth in the sand with geogrid reinforcement in two layers in the horizontal direction that is at the top of the container and bottom of the container of soil at different density

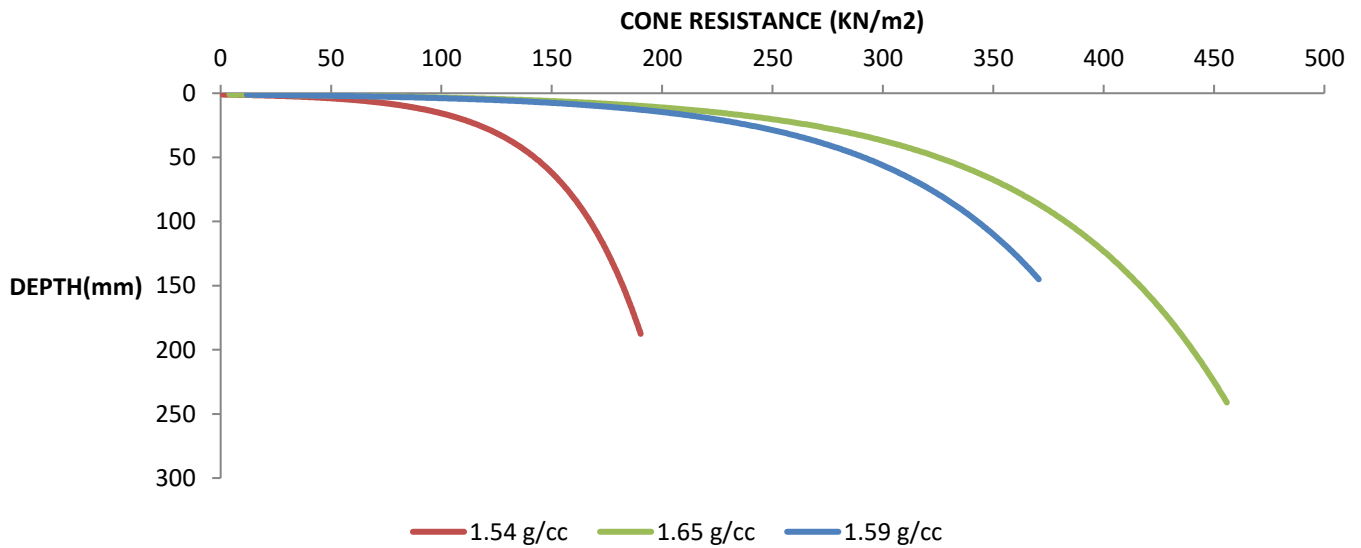


Figure 17: cone resistance profiles in the sand with reinforcement of geogrid in the horizontal direction at the top layer and bottom layer of soil layer at a different density.



Result: Cone resistance obtained is the highest for the soil with the highest density and is about 2.4 times to that of the soil with the lowest density.

4.5. The tabular form of Cone resistance with varying densities and varying orientation of geogrid

Density (g/cc)	Cone Resistance (KN/m <sup>2</sup> )		
	Sand without geogrid reinforcement	Sand with reinforced geogrid at the top, middle, and bottom layer	Sand with reinforced geogrid at top and bottom layer
1.54	95	166.4	191.2
1.59	126	317	370.6
1.65	208	376.5	455.8

Table 5: Cone penetration resistance with varying densities and varying orientation of geogrid

## Chapter 5

### Software Modeling

As stated earlier, the experiments were conducted to determine the cone penetration resistance of the soil. The sample of sand was taken, filled in a container of the above-mentioned size, and cone penetration resistance of soil using a static cone penetrometer was determined at a different density of soil. Out of which, it was further concluded that the highest value of resistance was offered by the soil at its dry density that is at a density of 1.65g/cc

Further, the geogrids reinforcement is used in horizontal orientation at different locations along with the height of the container. Two types of geogrid reinforcements were used in the experiment: these were the two-layer and a three-layer reinforcement and the value of penetration resistance was calculated and compared. The different locations that were used in the analysis were as follows:

- The soil sample without reinforcing the geogrid
- The soil sample with the geogrid reinforcement in three layers that is at the surface of the soil, at the mid-depth of 5.5cm, and the bottom of the container to a depth of 11 cm.
- The soil sample with the geogrid reinforcement in two layers that is at the surface of the soil and the bottom of the container to a depth of 11 cm.

In the analytical modeling, the experiment of cone penetration resistance was conducted at three different densities [1.54 g/cc, 1.59 g/cc, and 1.65 g/cc]. Out of these three different densities, it was observed in experimental research that the highest value of cone penetration resistance was being observed at a density of 1.65 g/cc in each of the three orientation arrangements of geogrids. Thus for the analysis using numerical modeling, the density of 1.65 g/cc is being selected to work for numerical modeling in the finite element model. To validate these results obtained by the analytical analysis, similar numerical modeling was being conducted using the finite element method (FEM) software PLAXIS 8.6. In which at the same value of the factored load.

The corresponding displacement and penetration resistance was calculated and compared with the previous analytical results. This comparison of analytical and numerical modeling results is defined by a dimensionless cone penetration resistance factor(DCPRF) which is being defined

as the ratio of the cone penetration resistance observed in analytical modeling to the cone penetration resistance observed in numerical modeling.

$$DCPRF = \frac{\text{conepenetrationresistanceinanalyticalmodeling}}{\text{conepenetrationresistanceinnumericalmodeling}}$$

### 5.1. Objective

The determination of the displacement caused by the cone in the soil layers and the cone penetration resistance value in terms of mean total stresses in the soil by using a finite element model (FEM) software PLAXIS 8.6. These values of displacement and penetration resistance were being further compared with the analytical results and suitable conclusions are being drawn.

### 5.2. Model Preparation

A similar model as being prepared for the analytical analysis was being prepared and being tested for on the software. The 2D analysis is being carried out by preparing a 2D block of sand of dimension 30cm in length and 12 cm in height.

A 15-noded axis-symmetry model mesh is prepared. In the generation of mesh, the cluster is divided into a set of triangles. The 15 node elements triangle is prepared to provide a better calculation of stresses and failure loads. In considering the same element distribution, the meshes composed of 15 nodes element is much finer and flexible than a 6 nodes geometry.

### 5.3. Modeling Analysis

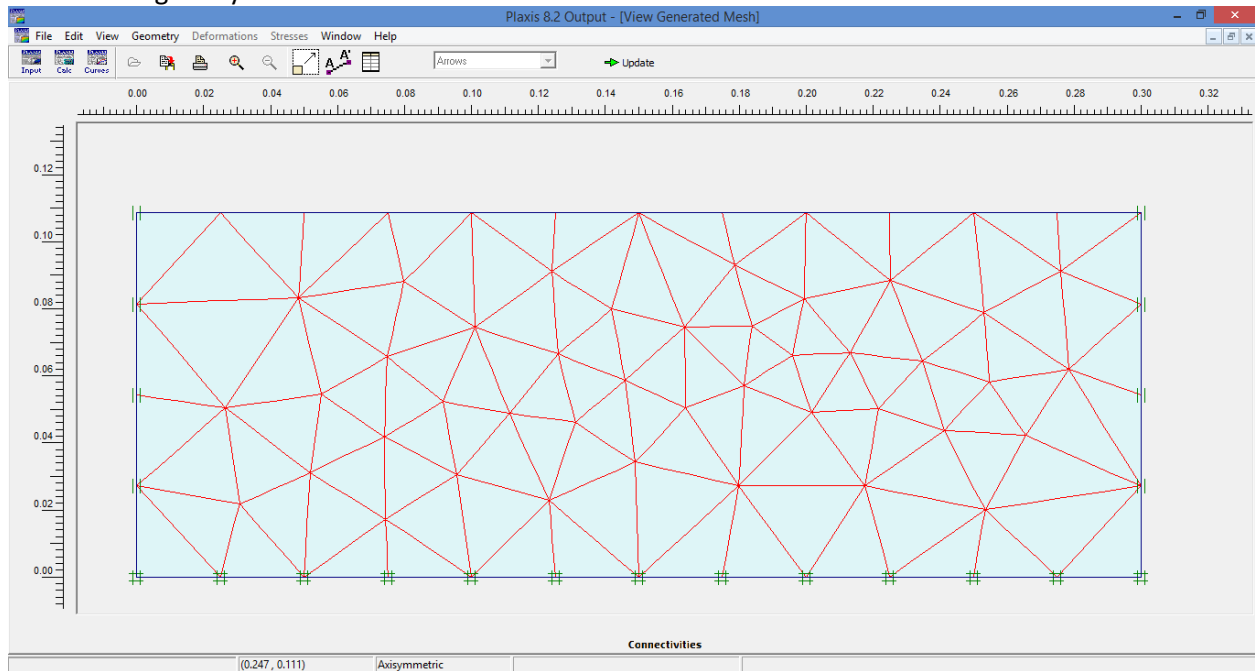


Figure18:A 15 noded Axis-symmetry model generated mesh

The following different conditions are considered.

1. The soil sample without placing the geogrid

The following soil sample is generated.

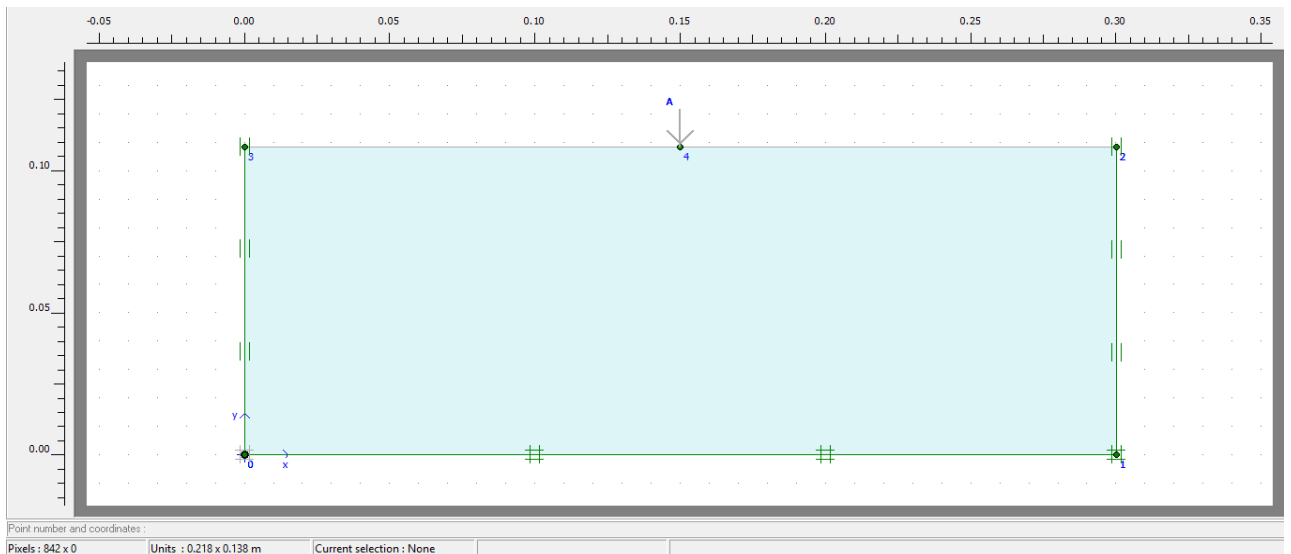


Figure 19: A soil element without geogrid reinforcement

From the analytical results, it was concluded that this soil sample failed at a failure load of 52.2Kg. Thus this load is being converted into the equivalent value of KN/m as

$$\text{Failure load in KN/m} = \frac{52.2 * 9.81}{1000 * 0.035} = 14.63 \text{ KN/m}$$

Since this failure load as used in the analytical analysis was a load applied at the cone, thus make this as equivalent, shape factor comes into consideration.

The shape factor of a cone of diameter D and height H is given by

$$SF = 1 - D / (\sqrt{4D^2 + H^2}) \text{ [et. al. Chung, Kermani and Naraghi]}$$

$$\text{Shape factor} = 1 - 3.5 / \sqrt{4 * 3.5^2 + 4.2^2} = 0.571$$

$$\text{Ultimate load} = 14.63 / 0.571 = 25.61 \text{ KN/m}$$

## Output of analysis

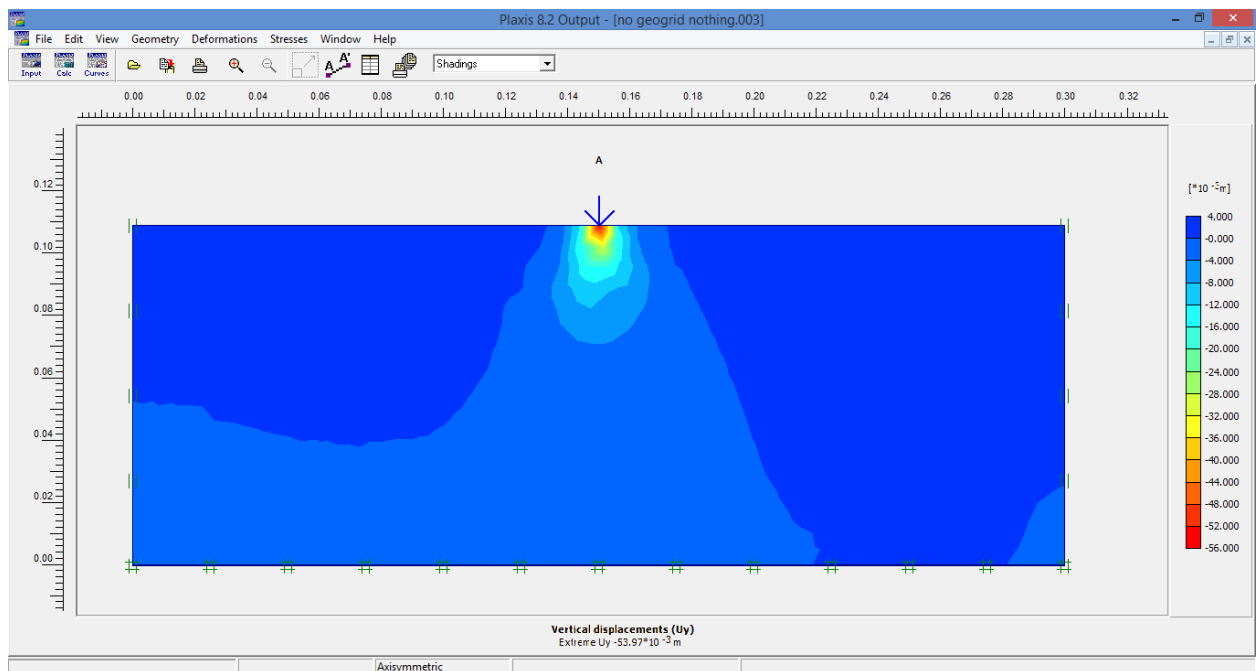


Figure 20: A plot of vertical displacement for a soil element without geogrid reinforcement

The figure shows the ultimate vertical displacement of 53.97 mm that is almost equal to one observed in the analytical analysis (62.4mm). This value of displacement is nearly the same because since the soil is not reinforced and all the conditions are kept the same. There is also a minor difference because exact numerical modeling conditions cannot be maintained at the practical analysis and vice versa

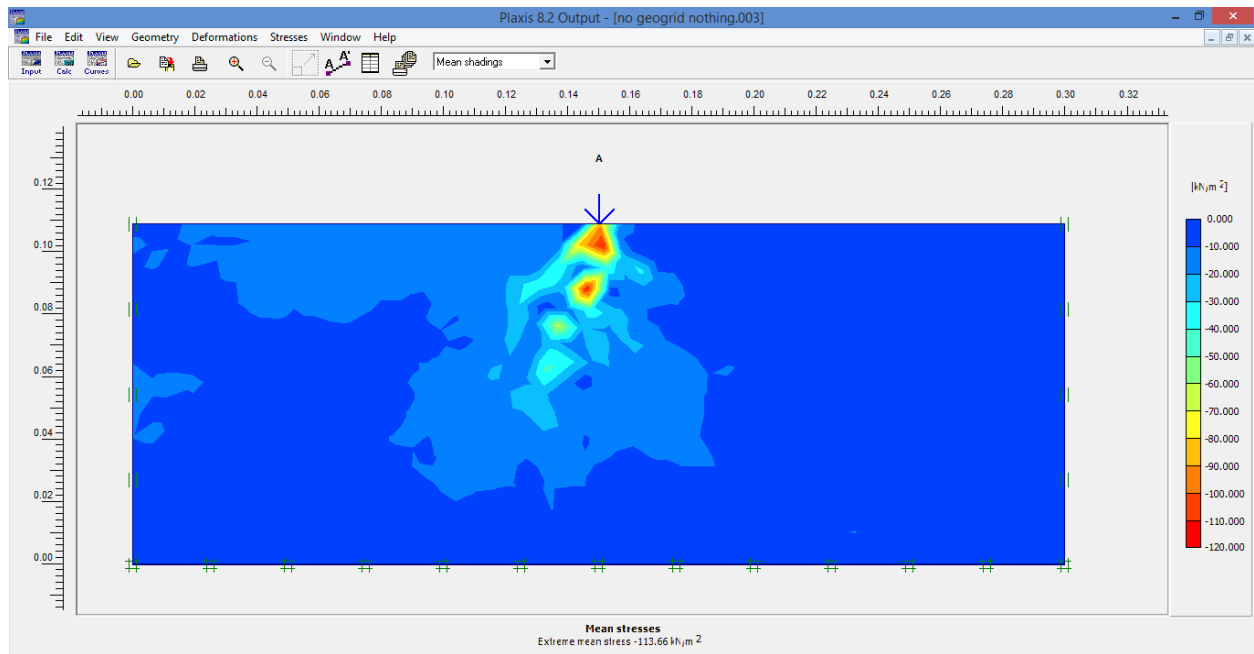


Figure 21: A plot of cone penetration resistance for a soil element without geogrid reinforcement

The effective principal stresses generated is of the order of 113.97 kN/m<sup>2</sup> that is very much less than that compared from the analytical analysis value of 208 kN/m<sup>2</sup>. There is also a difference because exact numerical modeling conditions cannot be maintained at the practical analysis and vice versa.

2. The soil sample with the two-layer geogrid reinforcement is geogrid placed in two layers that is at the surface of the soil and the bottom of the container to a depth of 11 cm.

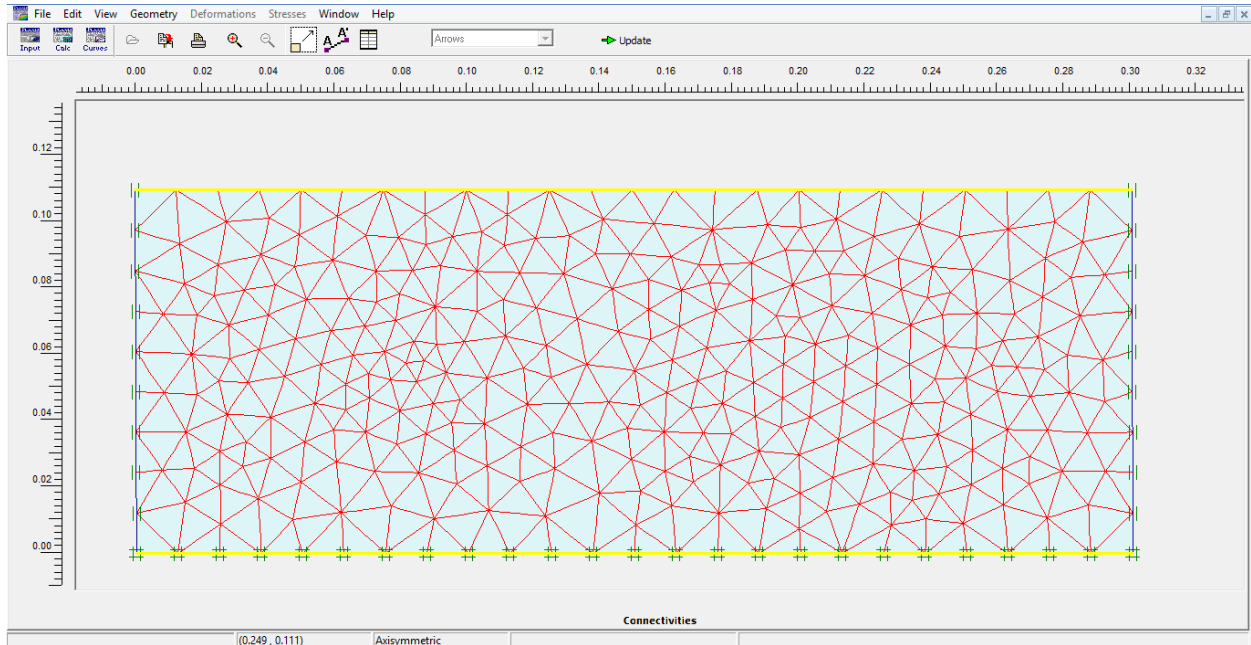


Figure 22: A soil element with a two-layer geogrid reinforcement

From the analytical results, it was concluded that this soil sample failed at a failure load of 115Kg. Thus this load is being converted into the equivalent value of KN/m as

$$\text{Failure load in KN/m} = \frac{115 * 9.81}{1000 * 0.035} = 32.23 \text{ KN/m}$$

Since this failure load as used in an analytical analysis was a load applied at the cone, thus to make this as equivalent, shape factor comes into consideration.

The shape factor of a conical of diameter D and height H=  $1 - D / (\sqrt{4D^2 + H^2})$

$$\text{Shape factor} = 1 - 3.5 / \sqrt{4 * 3.5^2 + 4.2^2} = 0.571$$

$$\text{Ultimate load} = 32.23 / 0.571 = 56.45 \text{ KN/m}$$

## Output of analysis

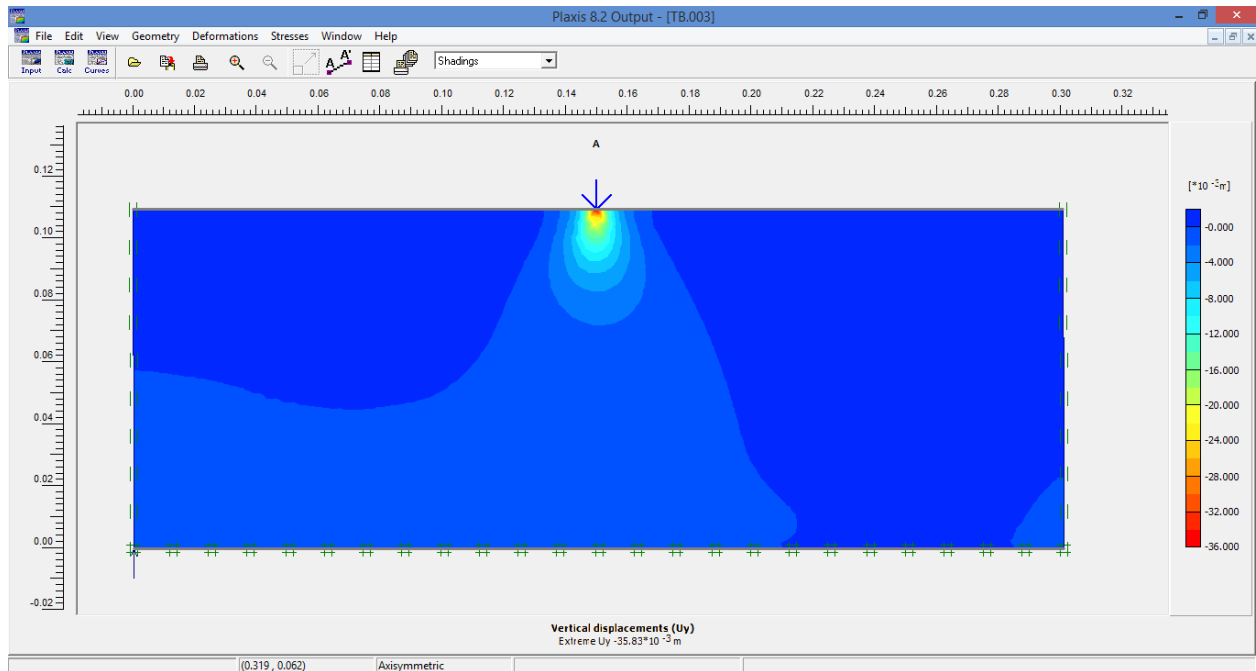


Figure 23:A plot of vertical displacement for a soil element with a two-layer geogrid reinforcement

the figure shows the ultimate vertical displacement of 35.83mm that is less than that observed in the analytical analysis (49.3mm). There is a minor difference because exact numerical modeling conditions cannot be maintained at the practical analysis and vice versa



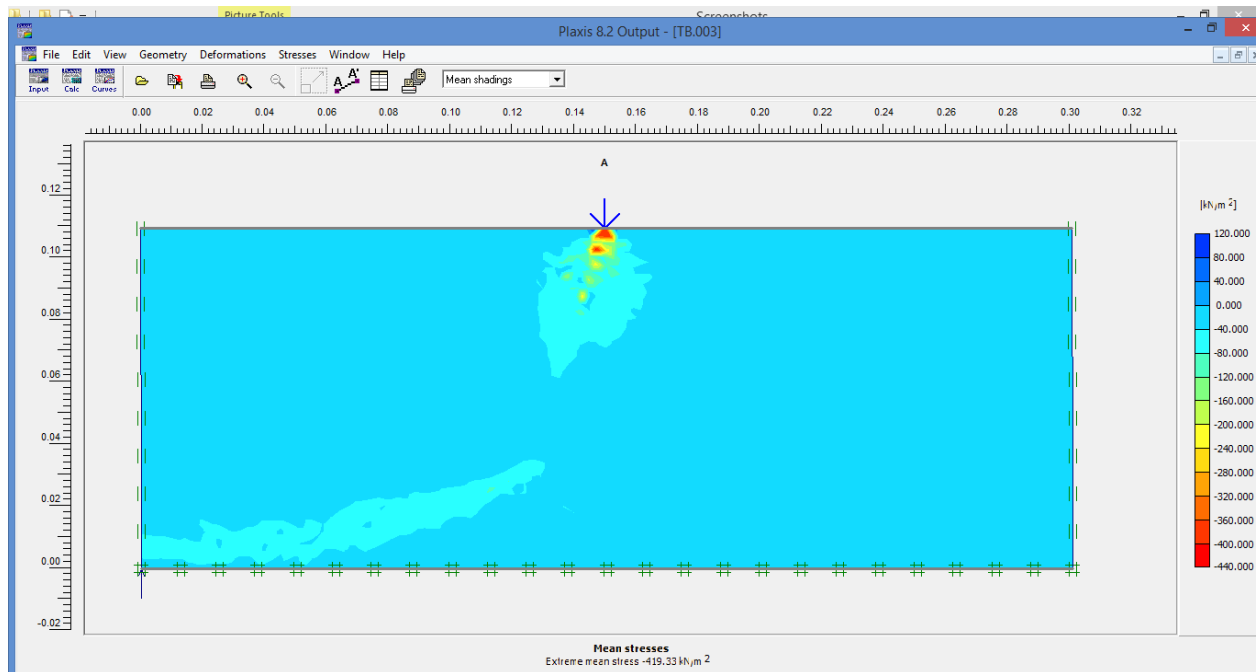


Figure 24: A plot of cone penetration resistance for a soil element with a two-layer geogrid reinforcement

The effective principal stresses generated is of the order of  $419.33 \text{ kN/m}^2$  that is almost equal to that compared from the analytical analysis value of  $456.8 \text{ kN/m}^2$

3. The soil sample with the soil reinforced with geogrid in three layers that are at the surface of the soil, at the bottom of the container to a depth of 11 cm, and the mid-depth of the soil sample to a depth of 5.5 cm from top.

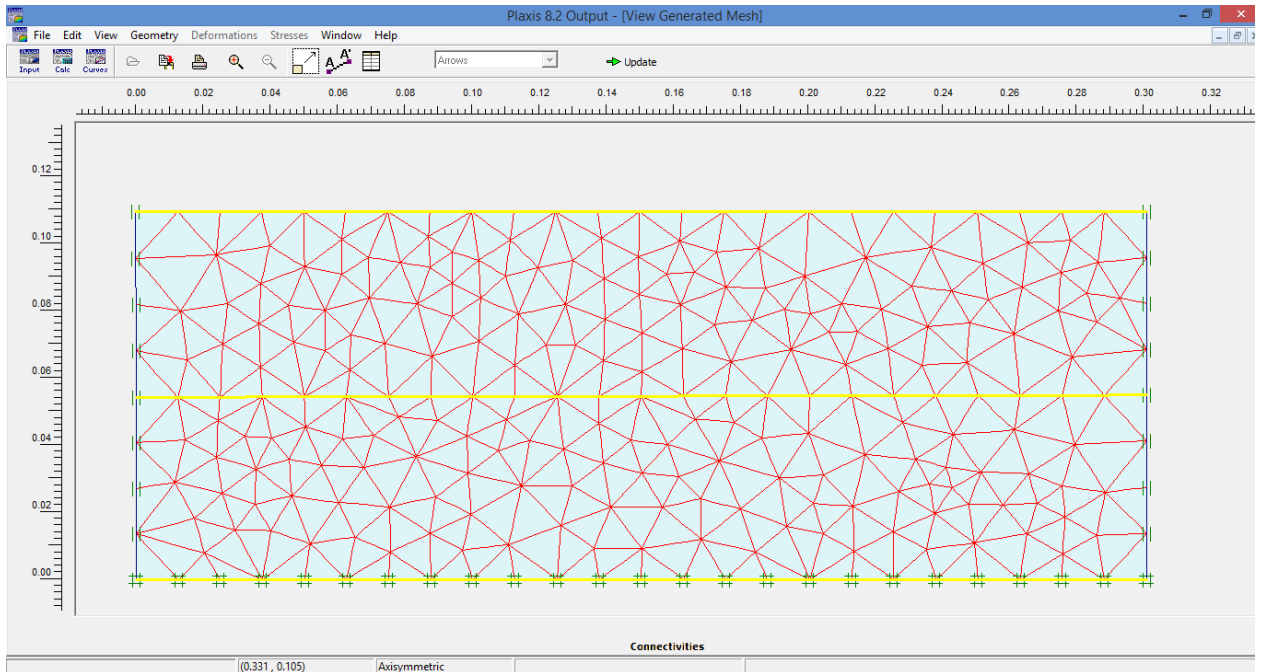


Figure 25: A soil element with a three-layer geogridsreinforcement

From the analytical results, it was concluded that this soil sample failed at a failure load of 95Kg. Thus this load is being converted into the equivalent value of KN/m as

$$\text{Failure load in KN/m} = \frac{95 * 9.81}{1000 * 0.035} = 26.627 \text{ KN/m}$$

Since this failure load as used in an analytical analysis was a load applied at the cone, thus to make this as equivalent, shape factor comes into consideration.

The shape factor of a conical of diameter D and height H=  $1 - D / (\sqrt{4D^2 + H^2})$

$$\text{Shape factor} = 1 - 3.5 / \sqrt{4 * 3.5^2 + 4.2^2} = 0.571$$

$$\text{Ultimate load} = 26.627 / 0.571 = 46.631 \text{ KN/m}$$

## Output of analysis

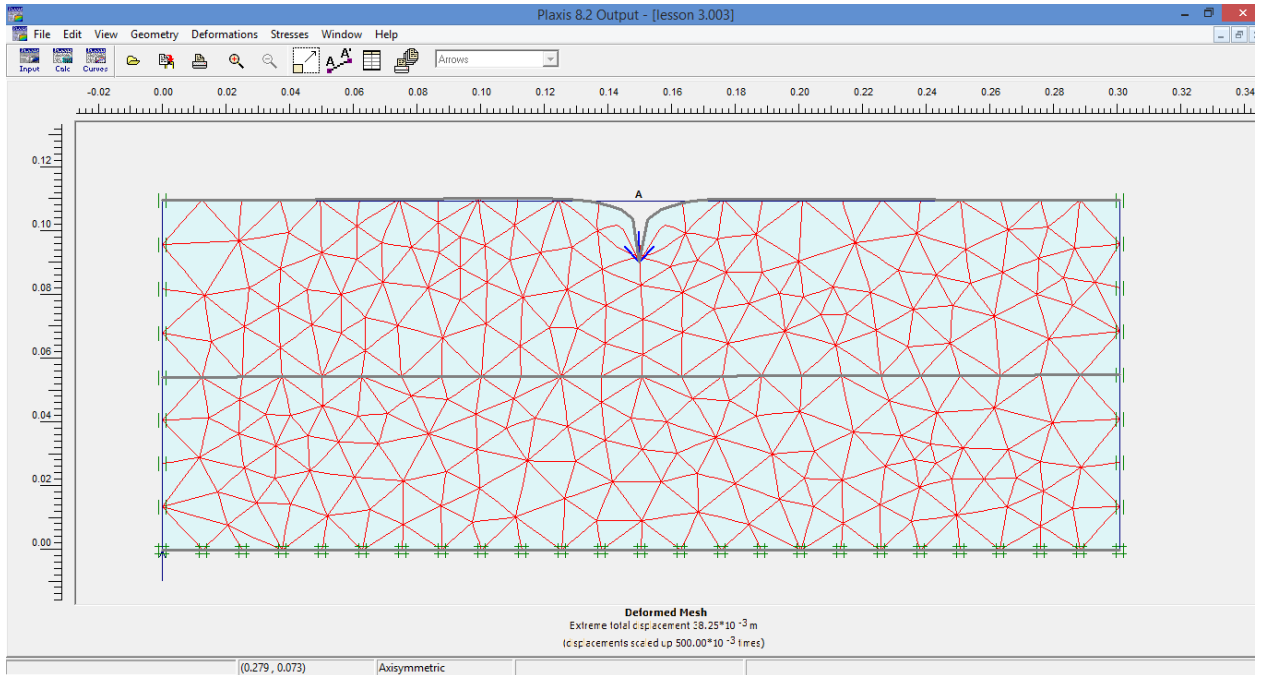


Figure 26: plot of a deformed mesh for a three-layer geogrid reinforced soil element

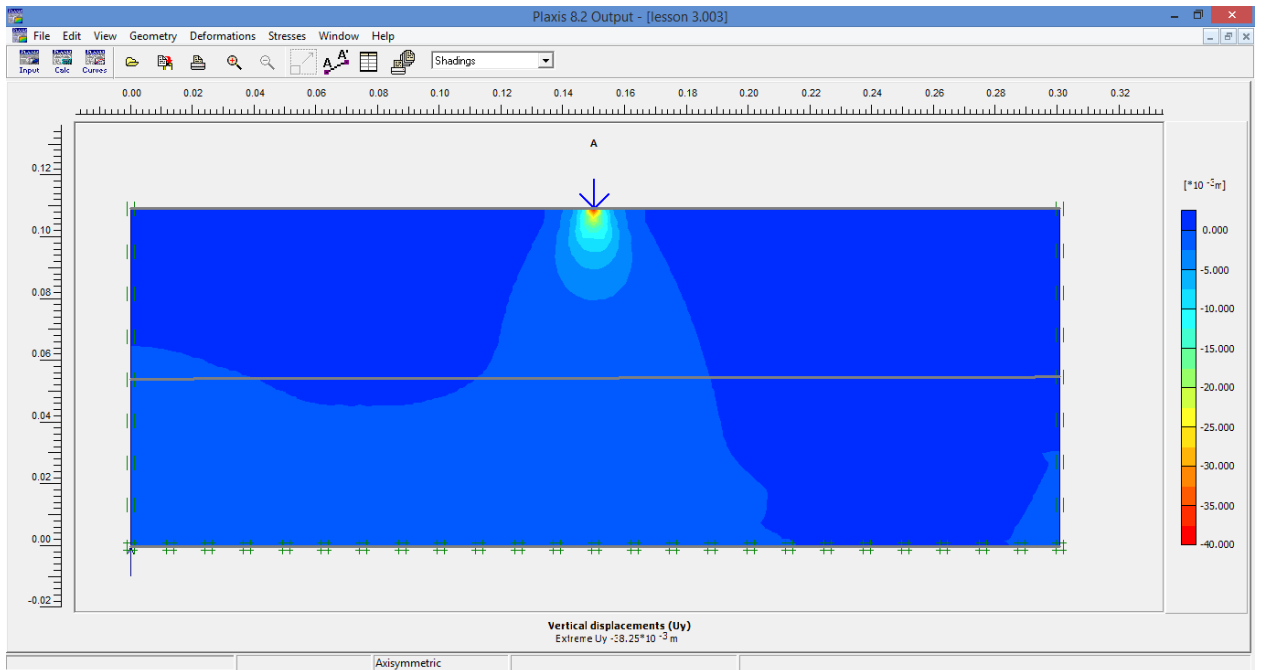
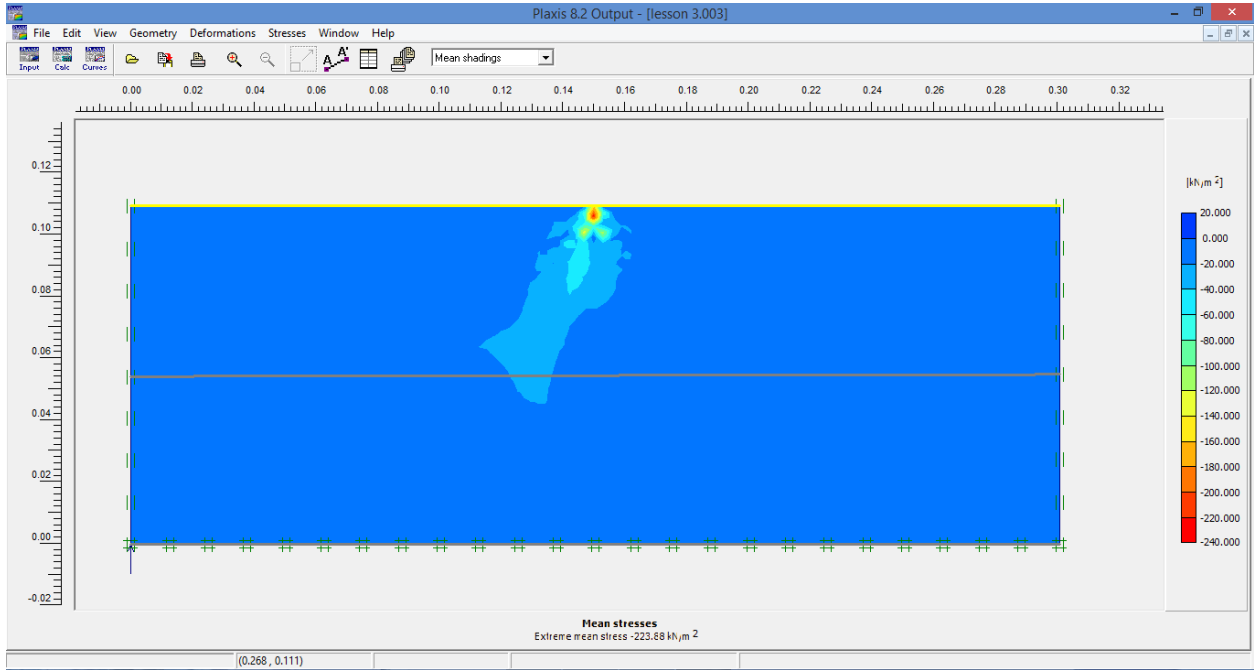


Figure 27: A plot of vertical displacement for a soil element with a three-layer geogrid reinforcement

the figure shows the ultimate vertical displacement of 38.25mm that is less than that observed in the analytical analysis (45.3 mm).



**Figure 28:**A plot of cone penetration resistance for a soil element with a three-layer geogrid reinforcement

The effective principal stresses generated is of the order of 223.68 kN/m<sup>2</sup> that is less than that compared from the analytical analysis value of 350 kN/m<sup>2</sup> There is also a minor difference because the exact numerical modeling conditions cannot be maintained at the practical analysis.

5.4. Table of comparison of results in numerical modeling and analytical modeling and its related Graphs

Soil arrangement Factored load (KG)		Displacement (mm)	
		Numerical modeling	Analytical modeling
Soil without geogrid reinforcement	52.2	53.97	62.4
Soil with reinforced geogrid in three layers	115	35.83	49.3
Soil reinforced with geogrid in two layers	95	38.25	45.3

Table 6: Tabular form of Load and Displacement in numerical and analytical modeling

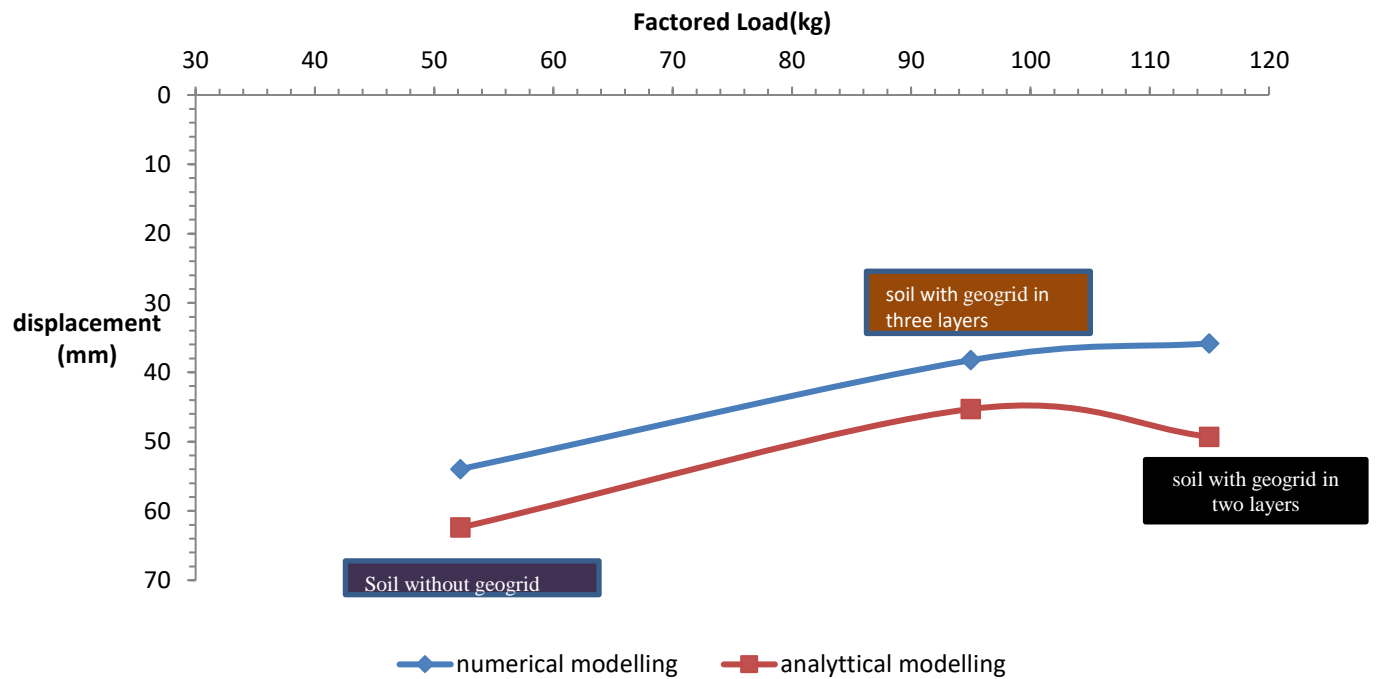


Figure 29: Comparison of load Vs displacement for numerical and analytical modeling for different orientation of geogrid reinforcement

Soil arrangement Factored load (KG)		Cone penetration resistance (kN//m <sup>2</sup> )	
		Numerical modeling	Analytical modeling
Soil without geogrid reinforcement	52.2	113.97	208
Soil with reinforced geogrid in three layers	95	223.68	350
Soil reinforced with geogrid in two layers	115	419.33	456.8

Table 7: Tabular form of Load and cone penetration resistance in numerical and analytical modeling

**Comparison of load Vs cone penetration resistance for numerical and analytical modelling**

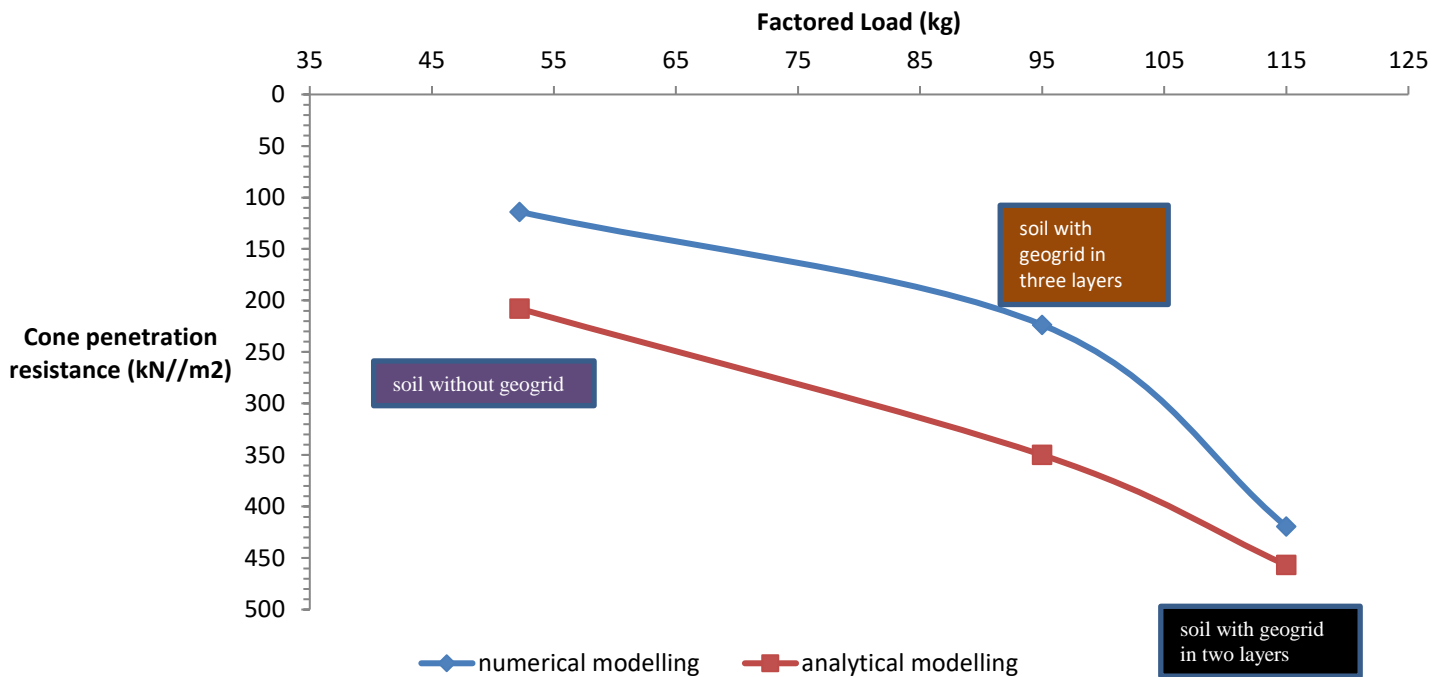


Figure 30: Comparison of load Vs cone penetration resistance in numerical and analytical modeling for different orientation of geogrid reinforcement

The cone penetration resistance values obtained in the analytical modeling and numerical modeling are compared by a dimensionless cone penetration resistance factor(DCPRF), which is defined as the ratio of the cone penetration resistance obtained in analytical modeling to that the cone penetration resistance obtained in numerical modeling.

Soil arrangement	Factored load (KG)	Cone penetration resistance (kN//m <sup>2</sup> )		DCPRF
		Numerical modeling	Analytical modeling	
Soil without geogrid reinforcement	52.2	113.97	208	1.825
Soil with reinforced geogrid in three layers	95	223.68	350	1.564
Soil reinforced with geogrid in two layers	115	419.33	456.8	1.089

Table 8: Tabular form of Load and DCPRF

The value of DCPRF is obtained as 1.825, 1.564, and 1.089 for the soil without geogrid, soil reinforced with geogrid in three layers, and soil reinforced with geogrid in two layers respectively. This shows that as the factored load is increased in the soil arrangement, the value of DCPRF converges to 1.

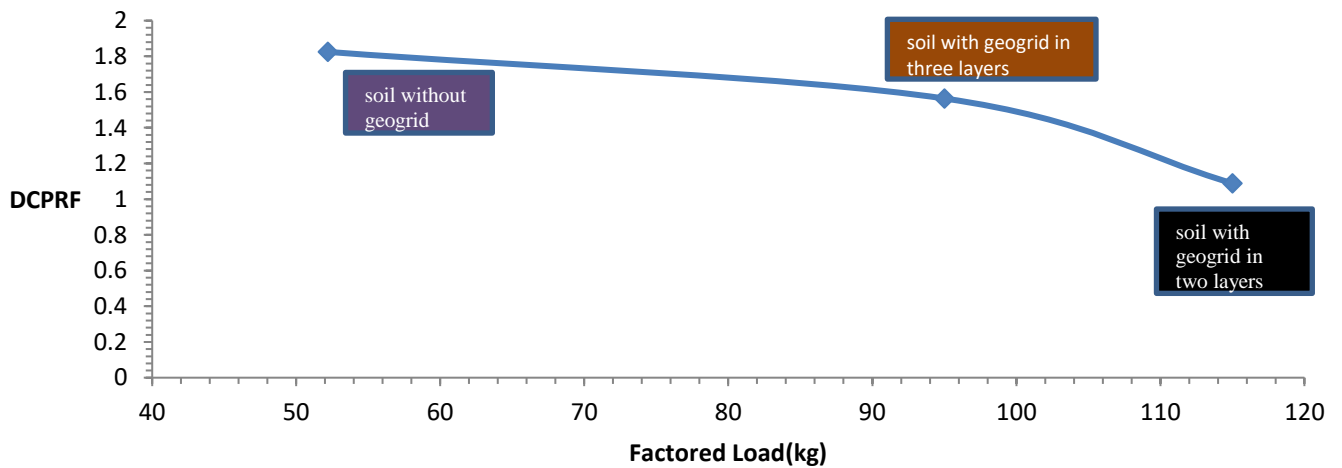


Figure 31: Comparison of load Vs DCPRF in numerical and analytical modeling for different orientation of geogrid reinforcement

## CHAPTER 6

### CONCLUSION

The following conclusions can be drawn from the study of cone penetration resistance in sand using the analytical approach and the auto-adaptive re-meshing finite model has been presented.

- The inclusion of geogrid in two layers reinforcement and three-layer reinforcement at varying depths in soil enhances the strength of soil in terms of cone penetration resistance of the soil.
- This inclusion of geogrid as reinforcement in the soil at different densities also yielded that with the increase in density, the cone penetration resistance of soil increases.
- The cone penetration resistance value increases by about 45% for a soil reinforced with geogrid in three layers as compared to the soil without reinforcement and this value of cone penetration resistance increases by a massive share of 120% for a soil reinforced with two-layer reinforcement at a density of 1.65 g /cc.
- Placing the geogrid in the double layer reinforcement yields the largest improvement regardless of the density.
- The optimum location of reinforcement was found to be at the top of the soil and depth of H for the dense sand.
- The difference in the numerical modeling results and the analytical modeling results are given by a means of a factor called DCPRF (dimensionless cone penetration resistance factor). This value of DCPRF converges to unity as the load on the soil specimen is increased.
- This convergence of DCPRF to unity clearly states that the cone penetration resistance analysis is validated by both numerical and analytical modeling.



## **FUTURE SCOPE**

- The effect of Different types of Geogrids used as a reinforcement in soil on Load V/s displacement characteristics and Load Vs cone penetration resistance can be studied.
- Different Configurations or orientations of Geogrids can be tried i.e. horizontal, vertical, inclined and its Load V/s Displacement characteristics and load Vs Cone penetration Characteristics can be studied.
- Spacing's of Geogrid can be varied and its effect on Load V/s Displacement characteristics and Load Vs Cone penetration Characteristics can be studied.
- The effect of Geogrid reinforcement in dynamic analysis using a moving load or a cyclic load can be studied and its effect on Load Vs displacement characteristics and Load Vs Cone Penetration resistance characteristics can be studied.
- This dynamic analysis can be linked with the road and rail traffic characteristics and can be implied with the construction of road pavements and railway ballast.

## REFERENCES

1. Indian Standard, "Method for sub-surface sounding for soils". IS:4968(part II)-1976
2. Lunne T, Robertson P.K, and Powell J.J.M.(1997), "Cone penetration testing in geotechnical Practice", Soil Mechanics and foundation engineering, Vol 46, No 6, 2009
3. Mcdowell G.R, and Bolton M.D. (2000) ,"Effect of particle size distribution on pile tip resistance in calcareous sand in the geotechnical Centrifuge," Granular matter-Springer , Vol 2, No 4, pp 179-187.
4. Mesri G, Feng TW, and Benak JM.,(1990) "Post densification penetration resistance of clean sand" Journal of Geotechnical Engineering, Vol. 116, No 7, pp. 1095-1115.
5. Qian Y, Hane J. ,Pokharal SK. and Parson RL.(2013) "Performance of Triangular Aperture Geogird Reinforced Base courses over weak sub grade under cyclic loading." Journal of Material in Civil Engginering, 25(8): 1013-1021.
6. Ranjan G, Rao A,(1991) "Basic and applied soil Mechanics", New Age International Publications.
7. Shinoda M. and Bathurst RJ,(2004)"Strain measurement of geogrids using a video-Extensometer technique" Geotechnical Testing Journal, Vol, 27, No 5, , pp 1-8.
8. Salgado R, (2014) "Experimental research on cone penetration resistance". Geo-Congress 2014 Keynote Lectures, GSP 235 © ASCE, pp. 140-163.
9. Susila E. and Hryciw R.D. , (2003) "Large displacement FEM modelling of the cone penetration test(CPT) in normally consolidated sand" International Journal for Numerical and analytical methods in Geomechanics, 27:585-602
10. Trivedi A and Singh Sundar,(2004 )"Cone resistance of compacted ash fill," Journal of Testing and Evaluation, Vol. 32, No. 6, ,pp. 429-437.